

Unlocking the Metalation Applications of TMP-powered Fe and Co(II) bis(amides): Synthesis, Structure and Mechanistic Insights

Alessandra Logallo, Lewis C. H. Maddock, Manting Mu, Lisa Gravogl, Na Jin, Marconi N. Peñas-Defrutos, Karsten Meyer, Max García-Melchor,* and Eva Hevia*

Dedicated to the memory of Professor Ian Manners

Abstract: Typified by LiTMP and TMPMgCl.LiCl, (TMP=2,2,6,6-tetramethylpiperidide), s-block metal amides have found widespread applications in arene deprotonative metalation. On the contrary, transition metal amides lack sufficient basicity to activate these substrates. Breaking new ground in this field, here we present the synthesis and full characterisation of earth-abundant transition metals M(TMP)₂ (M=Fe, Co). Uncovering a new reactivity profile towards fluoroarenes, these amide complexes can promote direct M–H exchange processes regioselectively using one or two of their basic amide arms. Remarkably, even when using a perfluorinated substrate, selective C–H metalation occurs leaving C–F bonds intact. Their kinetic basicity can be boosted by LiCl or NBu₄Cl additives which enables formation of kinetically activated ate species. Combining spectroscopic and structural studies with DFT calculations, mechanistic insights have been gained on how these low polarity metalation processes take place. M(TMP)₂ can also be used to access ferrocene and cobaltocene by direct deprotonation of cyclopentadiene and undergo efficient CO₂ insertion of both amide groups under mild reaction conditions.

Introduction

In the realm of s-block metal amide chemistry, 2,2,6,6-tetramethylpiperidide (TMP) occupies a privileged position on account of its widespread applications in selective deprotonative metalation reactions.^[1] Exemplified by LiTMP and its enhanced Turbo-Hauser base version TMPMgCl.LiCl, these amides combine low nucleophilicity with high

Brønsted basicity, ideal for selective cleavage of C–H bonds of aromatic substrates.^[2] The special electronics and architecture of the cyclic TMP group, featuring two methyl substituents on each *alpha* carbon atoms, not only amplifies its basicity but also significantly increases its steric demand.^[3]

Seminal work by Knochel, Mulvey, and Uchiyama amongst others has demonstrated the exceptional basicity of TMP when in bimetallic environments such as alkali-metal zincates, magnesiates and aluminates.^[4] The introduction of bimetallic cooperation in these systems not only enhances reactivity but also imparts unique selectivity that sets them apart from their monometallic counterparts.^[5] TMP seems to be complicit in this special bimetallic chemistry, since when replaced by other amide groups, diminished reactivities are often observed.^[6]

In contrast to these extensive main-group executed applications, TMP is much less visible in transition metal complexes, though a few sporadic studies of Fe and Co studies have hinted at their potential as arene metalators. Thus, Knochel has reported that *in situ* prepared Fe(TMP)₂.2MgCl₂.4LiCl, made by salt metathesis of FeCl₂.LiCl with 2 equivalents of TMPMgCl.LiCl, can metalate functionalized arenes to generate putative FeAr₂ species that subsequently undergo C–C bond formation processes (Figure 1a).^[7] However the identity of the Fe(II) amide and bis(aryl) intermediates remains blurred as do the roles played by LiCl or MgCl₂ in facilitating the possible formation of ferrate species. Similarly, Mongin has prepared *in situ* Co(TMP)₂ by treating CoBr₂ with LiTMP in THF which in combination with LiTMP can deprotonate a range of substituted anisoles (Figure 1b), though a large excess of

[*] Dr. A. Logallo,[†] Dr. L. C. H. Maddock,[†] N. Jin, Prof. Dr. E. Hevia
 Department für Chemie und Biochemie
 Universität Bern
 Freiestrasse 3, 3012 Bern (Switzerland)
 E-mail: eva.hevia@unibe.ch

M. Mu, Dr. M. N. Peñas-Defrutos, Prof. M. García-Melchor
 School of Chemistry, CRANN and AMBER Research Centres
 Trinity College Dublin
 College Green, Dublin (Ireland)
 E-mail: garciamm@tcd.ie

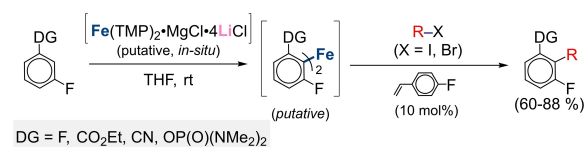
L. Gravogl, Prof. Dr. K. Meyer
 Department of Chemistry and Pharmacy,
 Inorganic Chemistry Friedrich-Alexander-Universität Erlangen-Nürnberg (FAU)
 Egerlandstraße 1, 91058 Erlangen (Germany)

Dr. M. N. Peñas-Defrutos
 IU CINQUIMA, Química Inorgánica,
 Facultad de Ciencias, Universidad de Valladolid,
 47071 Valladolid (Spain)

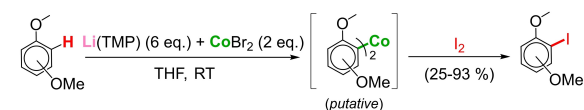
© 2024 The Authors. Angewandte Chemie International Edition published by Wiley-VCH GmbH. This is an open access article under the terms of the Creative Commons Attribution Non-Commercial NoDerivs License, which permits use and distribution in any medium, provided the original work is properly cited, the use is non-commercial and no modifications or adaptations are made.

Previous works

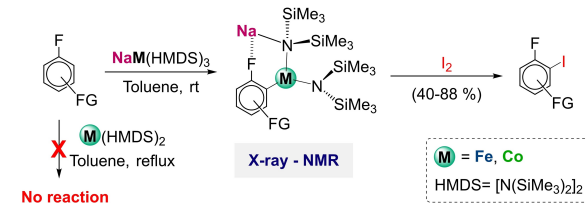
a) Knochel: Fe(II)-mediated ferrate cross coupling of functionalized arenes



b) Mongin: Co(II)-mediated deprotonative metalation of functionalized arenes



c) Hevia: Metalation of pentafluorobenzene via intramolecular sodium mediation



This work

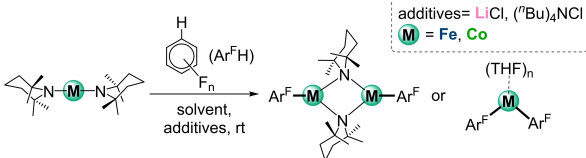
d) Direct metalation of fluoroarenes by M(TMP)₂ complexes

Figure 1. Applications of M(II)-bis(amide) complexes (M = Fe, Co) for arene deprotonative metalation.

base is needed. Moreover, neither the constitution of Co(TMP)₂ nor the mechanism(s) involved have been studied.^[8]

This lack of fundamental knowledge on the synthesis and constitution(s) of M(TMP)₂ (M = Fe and Co) is particularly surprising, especially in light of the well-established reports of Fe and Co bis(amide) complexes, such as M(HMDS)₂; (HMDS = N(SiMe₃)₂; M = Fe, Co), spanning over six decades.^[9] Significantly, while M(HMDS)₂ complexes have demonstrated their ability to act as versatile precursors of many M(II)/M(I) complexes,^[10] and to catalyze key transformations (such as hydrosilylation or alkyne trimerization processes), their ability to promote deprotonative metalation reactions has hitherto been limited to highly acidic substrates such as alcohols or secondary phosphines,^[11] being completely inert towards C–H arene bonds. Opening a new chapter in this literature, our groups recently found that pairing M(HMDS)₂ with sodium amide NaHMDS produced highly reactive sodium transition-(metal) ate complexes capable of promoting regioselective ferration and cobaltation of several fluoroarenes (Figure 1c).^[12] Mechanistic studies suggested that initially the fluoroarenes are metalated by the sodium amide followed by fast transmetalation to Fe (or Co) which can occur inter- or intra-molecularly.^[12a,c] Evidencing the poor metalating power of the TM amides M(HMDS)₂, no reaction was

observed when treated with pentafluorobenzene under harsh reaction conditions.

Filling an important knowledge gap, here we report the synthesis and full spectroscopic, electronic, and structural characterization of the transition metal bis(amides) M(TMP)₂ (M = Fe, Co) and explore their reactivity towards fluoroarenes, uncovering their metalating potential to promote direct low polarity metalations without aid of an alkali-metal (Figure 1d). Supported by DFT calculations, we shed light on the mechanisms involved in these reactions and on the role of additives such as LiCl, NBu₄Cl or Lewis donors such as THF, which not only enhance the metalating power of these new earth abundant transition metal amides but also show polybasic behaviours.

Results and Discussion

Approaching the synthesis of M(TMP)₂ via salt metathesis by treating FeBr₂ or CoCl₂ with two molar equivalents of LiTMP in THF at –30 °C (Figure 2aa, i) led to the formation of orange and green solutions respectively. Removing THF in vacuo, extracting with pentane and filtering through celite yielded a crude product that could be purified via dynamic vacuum distillation giving Fe(TMP)₂ (**1^{Fe}**) and Co(TMP)₂ (**1^{Co}**) as crystalline solids in respective 64 % and 46 % isolated yields. Interestingly, **1^{Fe}** and **1^{Co}** could also be obtained using trans(amidation) by reacting a 2:1 ratio NaTMP and M(HMDS)₂ mixture at –30 °C in pentane (Figure 2aa, ii). While **1^{Fe}** and **1^{Co}** are well soluble in pentane, the byproduct of the reaction NaHMDS forms as a precipitate that can be removed by filtration. [(THF)Co(TMP)₂] (**1^{Co}**-THF) could also be prepared via salt-metathesis by recrystallisation in THF (Figure 2a, iii, see Supporting Information for details).

Despite their paramagnetic nature, informative ¹H NMR spectra could be obtained in C₆D₆ for **1^{Fe}** and **1^{Co}** displaying three highly broadened and paramagnetically shifted resonances for the beta, gamma, and Me hydrogens of the TMP ligands at 169.97, 138.88, and 81.28 ppm, respectively, for **1^{Fe}** and at 186.95, 172.63 and 8.08 ppm, respectively, for **1^{Co}**. Molecular structures of **1^{Fe}** and **1^{Co}**-THF were established by X-ray crystallographic studies.^[13] Exhibiting a structure reminiscent of those of M(TMP)₂ (M = Zn, Cd),^[14,15] solvent-free **1^{Fe}** displays a rare monomeric arrangement (Figure 2aa),^[16] featuring an Fe(II) center in a gently bent distorted linear geometry [N1–Fe1–N2 angle, 172.09(14)°] which forms two short Fe–N bonds [1.875(3) and 1.871(3) Å]. The opposing TMP ligands are twisted in order to minimize repulsive steric interactions with a twist angle of 73.05(18)° between the C3–N1–C7 and C12–N2–C16 planes. In addition, four medium to long interactions are discernible between Fe and two α-Me groups from each TMP group [ranging from 2.886(5) to 2.953(3) Å] which may explain the slight deviation from linearity of the N1–Fe1–N2 angle. **1^{Co}**-THF features a distorted trigonal Co(II) center which binds terminally to two TMP groups [Co1–N1, 1.893(3); and Co1–N2, 1.884(3) Å] and one THF molecule. This motif is similar to that reported by Power for [(THF)Co(HMDS)₂]^[17]

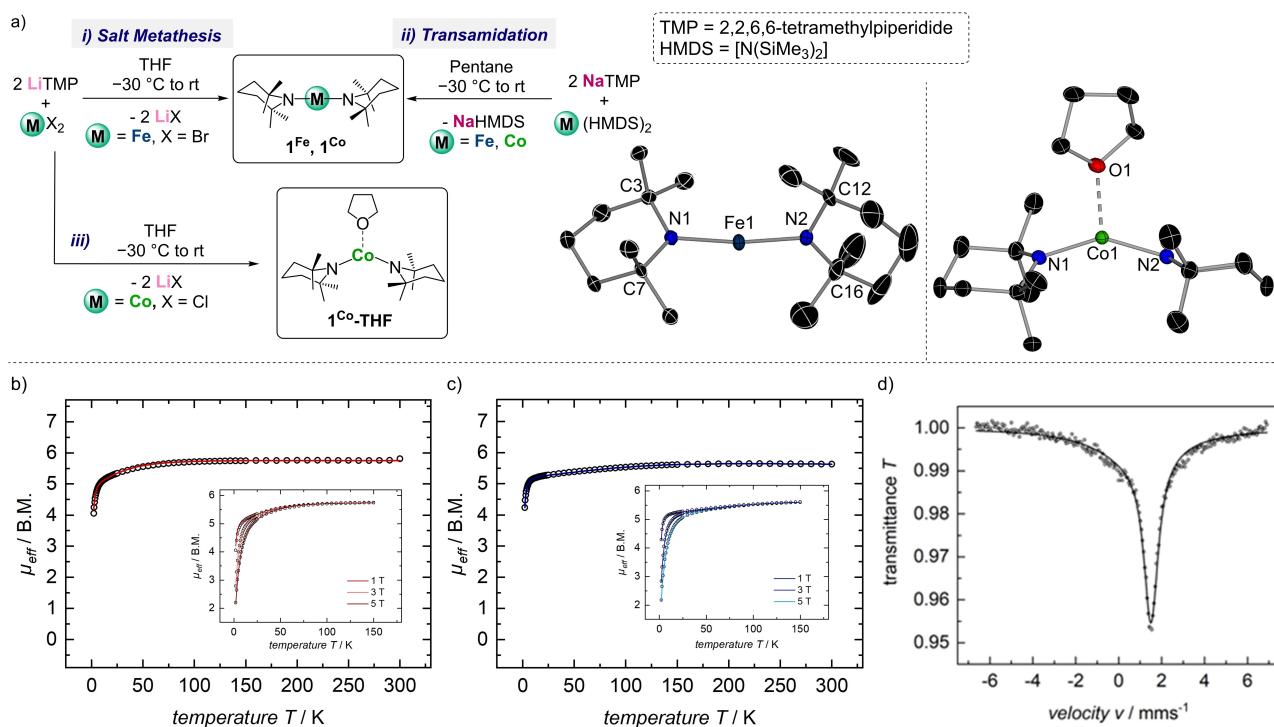


Figure 2. (a) Synthesis of $\text{M}(\text{TMP})_2$ ($\text{M} = \text{Fe}, \mathbf{1}^{\text{Fe}}$; $\text{M} = \text{Co}, \mathbf{1}^{\text{Co}}$) and $[\text{Co}(\text{TMP})_2(\text{THF})]$ ($\mathbf{1}^{\text{Co-THF}}$). Inset: Molecular structures of complexes $\mathbf{1}^{\text{Fe}}$ (LHS) and $\mathbf{1}^{\text{Co-THF}}$ (RHS). Hydrogen atoms and minor positional disorder omitted for clarity and displacement ellipsoids displayed at 50% probability level. (b) VT SQUID DC Field magnetization measurement of $\mathbf{1}^{\text{Fe}}$. The solid line represents the best global fit to the experimental data. μ_{eff} (300 K) = 5.76 B.M., μ_{eff} (2 K) = 4.05 B.M., $g_{\perp} = 2.27$, $g_{\parallel} = 2.48$ ($g_{\text{av.}} = 2.34$), $D = 28 \text{ cm}^{-1}$. Inset: VT SQUID DC Field magnetization measurement of $\mathbf{1}^{\text{Fe}}$, recorded from 2–150 K at 1, 3, and 5 T. The solid lines represent the best global fit to the experimental data. $g_{\perp} = 2.24$, $g_{\parallel} = 2.50$ ($g_{\text{av.}} = 2.33$), $D = -33 \text{ cm}^{-1}$; (c) Dark blue line: VT SQUID DC Field magnetization measurement of $\mathbf{1}^{\text{Co}}$, recorded from 2–300 K at 1 T. The solid line represents the best global fit to the experimental data. μ_{eff} (300 K) = 5.64 B.M., μ_{eff} (2 K) = 4.25 B.M., $g_{\perp} = 2.38$, $g_{\parallel} = 3.46$ ($g_{\text{av.}} = 2.79$), $D = -143 \text{ cm}^{-1}$. Inset: VT SQUID DC Field magnetization measurement of $\mathbf{1}^{\text{Co}}$, recorded from 2–150 K at 1, 3, and 5 T. The solid lines represent the best global fit to the experimental data. $g_{\perp} = 2.34$, $g_{\parallel} = 3.46$ ($g_{\text{av.}} = 2.76$), $D = -141 \text{ cm}^{-1}$; (d) Zero-field ^{57}Fe Mössbauer spectrum of $\mathbf{1}^{\text{Fe}}$ recorded at 77 K. $\delta = 1.16 \text{ mm s}^{-1}$, $\Delta E_Q = 0.68 \text{ mm s}^{-1}$, $\Gamma_{\text{whm}} = 4.42 \text{ mm s}^{-1}$, $w_{1/2} = 0.18$ (black). Data set was collected on a solid sample.

though a slightly more obtuse N–Co–N angle is seen in $\mathbf{1}^{\text{Co-THF}}$ [$145.48(13)^\circ$] most likely due to the greater steric demands imposed by TMP. As far as we can ascertain, $\mathbf{1}^{\text{Co-THF}}$ represents the first example of a structurally defined complex containing a TMP group bonded to Co.^[18]

The solid-state variable temperature, variable field (VTVF) SQUID magnetization data for $\mathbf{1}^{\text{Fe}}$ (Figure 2b) and $\mathbf{1}^{\text{Co}}$ (Figure 2c) show large room temperature magnetic moments of $\mu_{\text{eff}} = 5.76 \text{ B.M.}$ and 5.64 B.M. . It must be noted, however, that both complexes significantly exceed the spin-only values for $S = 2$ and $S = 3/2$ spin systems of 4.90 B.M. and 3.87 B.M., respectively, which is attributed to unquenched orbital angular momentum in linear coordination compounds, resulting in magnetic anisotropy.^[19] Regardless, both data sets could be fitted with the spin-only Hamiltonian, giving large anisotropic g -values. For $\mathbf{1}^{\text{Fe}}$, the best fit obtained for the VT SQUID data yields g -values of $g_{\perp} = 2.24$ and $g_{\parallel} = 2.50$, and a zero-field splitting parameter $D = -33 \text{ cm}^{-1}$ ($g_{\text{av.}} = 2.33$). The magnetic characteristics of $\mathbf{1}^{\text{Fe}}$ are commonly observed in linearly coordinated Fe(II) high-spin compounds.^[20] Additionally, the ^{57}Fe Mössbauer spectrum of $\mathbf{1}^{\text{Fe}}$ (Figure 2d) displays a notably asymmetric, broadened single line at 77 K. This is likely due to unresolved magnetic hyperfine and quadrupole splitting,

which can be observed for other linear Fe(II) high-spin complexes and is rationalized as a result of fast relaxation processes.^[21] As found for comparable linear Fe(I)^[19b,22] or Co(II) complexes,^[19c,23] the d^7 configuration of $\mathbf{1}^{\text{Co}}$ leads to even larger axial anisotropy, reflected by $g_{\perp} = 2.34$, $g_{\parallel} = 3.46$, and $D = -141 \text{ cm}^{-1}$ as obtained by fitting the VT SQUID magnetization data. Finally, $\mathbf{1}^{\text{Fe}}$ and $\mathbf{1}^{\text{Co}}$ show slow magnetic relaxation at low temperatures (see Supporting Information for details).

We started reactivity studies using pentafluorobenzene and 1,2,4,5-tetrafluorobenzene as model substrates. While their aromatic hydrogens are activated towards deprotonative metalation (in terms of $\text{p}K_{\text{a}}$ values)^[24] their high degree of fluorination makes them more prone to undergo C–F bond activation processes, especially in reactions with low valent transition metal complexes.^[25] ^1H NMR monitoring of the reactions of equimolar amounts of $\mathbf{1}^{\text{Fe}}$ and $\mathbf{1}^{\text{Co}}$ with these perfluorinated substrates in C_6D_6 led to the almost instantaneous formation of $[[\text{M}(\text{TMP})\text{Ar}^{\text{F}}]_2]$ ($\text{Ar}^{\text{F}} = \text{C}_6\text{F}_5$, $\mathbf{2}^{\text{M}}$; $\text{C}_6\text{F}_4\text{H}$, $\mathbf{3}^{\text{M}}$; $\text{M} = \text{Fe}, \text{Co}$) in quantitative yields with concomitant release of TMP(H), evidencing their metalating ability towards these substrates. Using pentane as solvent enabled isolation of $\mathbf{2}^{\text{M}}$ and $\mathbf{3}^{\text{M}}$ ($\text{M} = \text{Fe}, \text{Co}$) as crystalline solids (31–92% yield, see Supporting Information for details).^[26]

Emphasizing the enhanced basicity of these transition metal TMP complexes, their reactivity is in sharp contrast with the complete inertness of $M(\text{HMDS})_2$ amides towards these substrates, even under forcing refluxing conditions.^[12a,c] Importantly, while sodium ferrates (and cobaltates) $\text{NaM}(\text{HMDS})_3$ can promote fluoroarene metalations, it should be noted that these reactions occur by initial sodiation of the substrate followed by fast inter- or intramolecular transmetalation to Fe (or Co) (Figure 1c).

Structural studies revealed the dimeric structures of 2^{M} and 3^{M} featuring a central planar four-atom {MNMN} core with TMP bridges, whereas the aryl groups bind terminally to the M^{II} centers (Figures 3 and S66–S69). For brevity, only the main structural parameters of 2^{Fe} and 2^{Co} are discussed here.

Confirming successful M–H exchange, 2^{Fe} and 2^{Co} contain a pentafluorophenyl anion bound terminally to either a Fe(II) or a Co(II) center via the metalated *ipso* C atom (average M–C bond length, 2.043 and 1.991 Å for 2^{Fe} and 2^{Co} respectively). These aromatic rings lie orthogonal to the plane of the {MNMN} central core, with the divalent metals exhibiting a distorted trigonal planar geometry. One noticeable feature of these structures is their metal-metal distances [2.5128(4) and 2.4221(5) Å for 2^{Fe} and 2^{Co} respectively], which are remarkably short when compared with those reported for other dimeric Fe(II) and Co(II) complexes containing amide or alkyl bridges.^[27] As far as we can ascertain, 2^{M} and 3^{M} represent the first examples of direct ferration and cobaltation of fluoroarenes to be isolated and structurally authenticated. While low-valent Fe and Co complexes have been previously used for functionalization of fluoroarenes, via C–H or C–F bond activation processes, these reactions typically occur with a change in the oxidation state of the metal.^[25,28] Remarkably, the

reactivities displayed by 1^{Fe} and 1^{Co} align better with those reported for main-group bases.^[29]

Variable temperature SQUID measurements were recorded for dinuclear 2^{Fe} and 2^{Co} . Both complexes show temperature-dependent magnetic moments. At 2 K, dimeric 2^{Fe} and 2^{Co} possess magnetic moments of $\mu_{\text{eff}}=0.34$ B.M and $\mu_{\text{eff}}=0.19$ B.M., reaching room temperature moments of 3.30 B.M and 1.95 B.M., respectively. This is far below the calculated magnetic moments of 6.93 B.M. (for Fe(II) high-spin) and 5.47 B.M. (Co(II) high-spin) for two uncoupled metal centers and therefore, suggests antiferromagnetic exchange coupling between the two metal ions. The ^{57}Fe Mössbauer spectrum of a solid sample of 2^{Fe} at 77 K (Figure S101) features a single quadrupole doublet with an isomer shift $\delta=0.63$ mms^{-1} and a large quadrupole splitting $\Delta E_{\text{Q}}=4.22$ mms^{-1} . Consistent with antiferromagnetic coupling, the resonances in the ^1H NMR spectrum for 2^{M} and 3^{M} in C_6D_6 are sharp and well resolved although they appear at chemical shifts typical for paramagnetic species.^[27c] In addition, meaningful ^{19}F NMR spectra could also be acquired (see Figures S9–S15).

We next pondered if the remaining TMP group present in 2^{M} and 3^{M} could facilitate the metalation of a second equivalent of substrate. ^1H NMR monitoring of the reactions showed that in C_6D_6 no further reactivity was observed even under forcing reaction conditions (16 h, 80 °C). However, when switching to more polar d_8 -THF, in the case of 2^{Fe} we could see formation of amine TMP(H) producing bis(aryl) [(THF)₂Fe(C₆F₅)₂] (4^{Fe}-THF) quantitatively (Figure 3). 4^{Fe}-THF could also be prepared by reacting 1^{Fe} with 2 equivalents of pentafluorobenzene using THF as solvent and isolated as a solid in a 98 % yield. Remarkably, 1^{Co} failed to exhibit polybasicity towards an excess of pentafluorobenzene in THF, even under refluxing conditions, forming exclusively 2^{Co} . The constitution of 4^{Fe}-THF was established by X-ray crystallographic studies (Figure 3), revealing a discrete centrosymmetric monomeric motif with Fe in a distorted tetrahedral geometry (bond angles range 116.47(9)–109.33(8)°). The Fe–C bond length [2.0863(17) Å] is slightly elongated to that previously noted in 2^{Fe} . Interestingly, bis(aryl)iron compounds have previously been proposed to be key intermediates in Fe-catalysed cross-coupling reactions.^[30] Recent mechanistic studies have accessed these compounds by salt metathesis using ArMgX and Fe(II) or Fe(III) salts.^[31] While Knochel et al. used $\text{Fe}(\text{TMP})_2 \cdot 2\text{MgCl}_2 \cdot 4\text{LiCl}$ as a base and suggested the *in situ* formation of such compounds (see Figure 1a),^[7] 4^{Fe}-THF stands out as a unique example of a FeAr_2 complex obtained by the direct metalation of an arene. ^1H NMR of 4^{Fe}-THF in C_6D_6 showed two paramagnetically shifted broadened signals at 42.6 and 16.90 ppm for the ligating THF molecules, whereas in the ^{19}F NMR spectrum only two signals could be seen at 145.7 and 15.5 ppm (see Supporting Information for details). Magnetic studies of the TMEDA solvated analogue of 4^{Fe} ($4^{\text{Fe}}\text{-TMEDA}$) were carried out and the data compared with the ones recorded for 1^{Fe} . While the averaged *g*-value, obtained from fitting the magnetization data of $4^{\text{Fe}}\text{-TMEDA}$, is similar, the zero-field splitting parameter is expectedly smaller compared to linear 1^{Fe} ($g_{\text{av}}=$

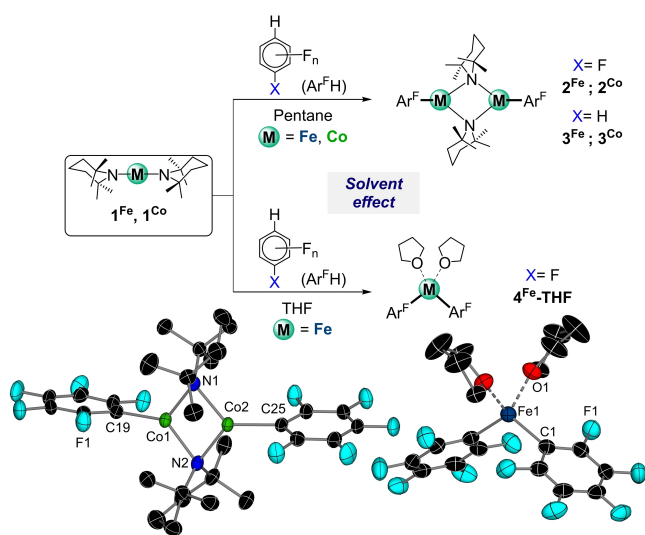


Figure 3. Reactivity of 1^{Co} and 1^{Fe} towards pentafluorobenzene and 1,2,4,5-tetrafluorobenzene. *Inset:* Molecular structures of complexes 2^{Co} and 4^{Fe}-THF . H atoms omitted for clarity and displacement ellipsoids displayed at 50% probability level.

2.32, $|D| = 7 \text{ cm}^{-1}$ for $4^{\text{Fe}}\text{-TMEDA}$ vs. $g_{\text{av}} = 2.31$, $D = -32 \text{ cm}^{-1}$ for 1^{Fe}). Notably, while the magnetization data of $4^{\text{Fe}}\text{-TMEDA}$ could be fitted with an averaged g -value, this was not possible for linear 1^{Fe} . Further, the zero-field ^{57}Fe Mössbauer data, with an isomer shift, δ , of 0.71 mm s^{-1} and a quadrupole splitting, ΔE_{Q} , of 1.74 mm s^{-1} , are in accordance with a tetrahedrally coordinated iron center with an $S = 2$ spin state (Figure S99).

Intrigued by the contrasting reactivities of 1^{Fe} and 1^{Co} toward pentafluorobenzene, we next conducted density functional theory (DFT) calculations at the ωB97XD level (see Supporting Information for details). As depicted in Figure 3, the iron complex demonstrates the ability to undergo the second C–H metalation, forming 4^{Fe}-THF . In contrast, the cobalt analogue exclusively yields the dimer 2^{Co} , ruling out any polybasic behavior.

The crucial role of reversible solvent molecule association in the thermodynamics of the process was experimentally suggested and confirmed by the coordination of solvent molecules in the solid state—either to the cobalt reactant $[(\text{THF})\text{Co}(\text{TMP})_2]$ (1^{Co}-THF) or to the iron product $[(\text{THF})_2\text{Fe}(\text{C}_6\text{F}_5)_2]$ (4^{Fe}-THF). Our initial speciation DFT studies on the $\text{M}(\text{TMP})_2$ complexes aimed to assess solvent coordination for the formation of the tricoordinate $[(\text{THF})\text{M}(\text{TMP})_2]$ species, using the implicit solvation model based on density (SMD, see Supporting Information for details). Endergonic association energies were obtained for both metal centers, i.e. $+5.5$ and $+1.2 \text{ kcal mol}^{-1}$ for iron and cobalt, respectively (Figure S84 and S85). These results contrast with the experimentally measured THF binding constants determined from ^1H NMR titrations (i.e. ${}^{\text{Fe}}K_{\text{eq}} = 0.44 \text{ M}^{-1} \pm 0.47\%$ vs ${}^{\text{Co}}K_{\text{eq}} = 113.61 \text{ M}^{-1} \pm 11.58\%$, Table S1),^[32] supporting a markedly favorable THF associa-

tion for cobalt. Additionally, significant formation of $[(\text{THF})\text{Fe}(\text{TMP})_2]$ (1^{Fe}-THF) was experimentally observed in THF solution. The substantial discrepancy is closely related to the high concentration effect of THF when acting as a solvent. In such cases, THF molecules surround the organometallic complexes, reducing the entropy penalty associated with their coordination and compromising the accuracy of traditional implicit solvation models.^[33] To realistically describe this scenario, we adopted a hybrid solvation method. This method integrates an explicitly modeled THF molecule within the computational framework, alongside implicit solvation corrections calculated via the SMD method, as illustrated in Figure S83. Specifically, the THF molecule is positioned in proximity to the metal complex and near the spectator TMP ligand without direct coordination to the metal, as depicted in Figure 4. This approach effectively cancels the translational contribution to the entropy cost required to bring the THF solvent molecule into the vicinity of the metal centre, thus providing a more precise representation.

Applying this hybrid strategy, THF dissociation from the $[(\text{THF})\text{M}(\text{TMP})_2]$ (1^{M}-THF) species was predicted to be endergonic for both metals, establishing these adducts as resting states of the linear $\text{M}(\text{TMP})_2$ (1^{M}) complexes in THF solution, consistent with experimental data. Specifically, cobalt exhibited a more disfavored THF dissociation compared to iron (i.e. $+1.1$ vs $+6.7 \text{ kcal mol}^{-1}$ for 1^{Fe} and 1^{Co} , respectively).

To rationalize this substantial difference, an activation strain analysis on the 1^{M}-THF adducts was subsequently performed. This involved defining $\text{M}(\text{TMP})_2$ and THF as molecular fragments and decomposing the relative energy of 1^{M}-THF into distortion (ΔE_{dist}) and interaction (ΔE_{int})

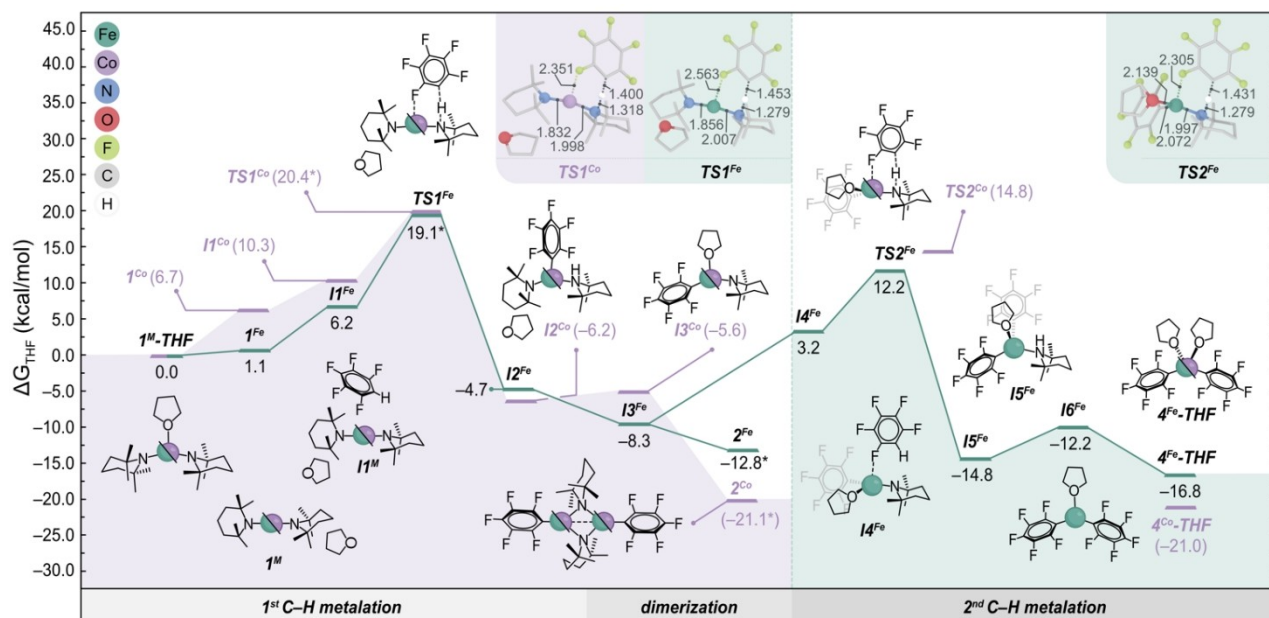


Figure 4. Gibbs energy profile calculated in THF at 298 K and 1 atm for the C–H metalation of C₆F₅H from the 1^M-THF complexes (M = Fe, Co, in green and purple, respectively) using a hybrid solvation model. Energies refined with microkinetic modelling are labelled with an asterisk. Relevant bond lengths (in Å) are shown for TS1^{Co}, TS1^{Fe} and TS2^{Fe}.

energy terms.^[34] The analysis revealed the cooperative effects of a lower ΔE_{dist} term in the cobalt fragment (compared to iron) and stronger ΔE_{int} between cobalt and THF (Table S6) as decisive factors for the higher preference of Co for THF binding (see Figure 2a).

In terms of metalating reactivity, the dissociation of THF from **1^M-THF** creates a vacant coordination on the metal center in **1^M**, essential for interaction with the C₆F₅H substrate to form **II^M**. The computed C–H metalation mechanism, illustrated in Figure 4, depicts similar structures for the resulting **II^M** intermediates with both metals. These structures exhibit weak interactions between the metal center and the aryl ring, with the fluoroarene hydrogen directed towards the nitrogen atom of one of the amide ligands.^[35] This particular arrangement facilitates C–H metalation via **TS1^M** with computed energies of +21.1 and +22.4 kcal mol⁻¹ for Fe and Co, respectively—well within the range of energies deemed to be feasible at room temperature. The above activation energies were further refined through microkinetic modelling (MKM) based on experimental observations (see Supporting Information for details), with the resulting values labelled with an asterisk in Figure 4. Notably, the estimated **TS1^{Co}** energy of 20.4 kcal mol⁻¹ is consistent with the major formation of the cobalt dimer **2^{Co}** observed experimentally within one hour at 298 K (Figure S93 and Table S7).

In addition, distinctive non-covalent interactions (NCI) between the metal center and one of the *ortho*-F substituents of the fluoroarene were observed for both **TS1^{Fe}** and **TS1^{Co}** (see Figure 4 for optimized structures with relevant distances and Figure S86 for NCI analyses), suggesting the role of fluorine as *ortho*-directing group in the C–H metalation process.

An alternative transition state to **TS1^M** was modelled maintaining the THF coordinated to the metal center, but it was discarded due to its higher energy (Figure S87). This finding strongly suggests the necessity of THF dissociation for the first metalation, a hypothesis that was experimentally confirmed. Specifically, solutions of the complex [(*i*Bu)Co(TMP)₂] (*i*Bu = 1,3-di-*tert*-butylimidazol-2-ylidene), prepared *in situ*, were unreactive towards pentafluorobenzene even under harsh conditions (16 h, 65°C; details in SI). This lack of reactivity is likely attributed to the non-lability of the carbene ligand, precluding the formation of the active linear complex **1^{Co}**, which is crucial for the interaction with the fluoroarene (Figure 4).

Geometry relaxations of the **TS1^M** structures resulted in the metalated intermediates **II^M** characterized by a covalent M–C₆F₅ bond and a protonated TMP(H) ligand coordinated to the metal center. Subsequent DFT calculations predict the substitution of the TMP(H) by a THF molecule to be exergonic for iron and slightly endergonic for Co (i.e. –3.6 and +0.6 kcal mol⁻¹, respectively), yielding the tricoordinate species [(THF)M(C₆F₅)(TMP)] (**II^M**).

This species, **II^M**, then undergoes dimerization to produce the antiferromagnetically coupled dimer [M(C₆F₅)(μ-TMP)]₂ (**2^M**) with the concomitant dissociation of THF for both iron and cobalt. The experimental magnetic moment of $\mu_{\text{eff}} = 0.34$ B.M. (Figure S106) and the greater

stabilization of **2^{Fe}** by –33.5 kcal mol⁻¹, compared to the ferromagnetically coupled dimer in a nonet high-spin state, further support the formation of this dimeric species.

To further refine the understanding of the thermodynamics and kinetics involved in the dimerization step, which encompasses double THF dissociation, MKM was employed. These ligand association/dissociation processes are known to be fast and often diffusion-controlled,^[36] posing challenges in locating the associated transition states. By integrating DFT and experimental data with MKM (see Supporting Information for complete kinetic model), we estimated the energy barrier for the dimerization process to be of +13.0 kcal mol⁻¹. Given the notable discrepancies in computational results typically obtained from different solvation methods in reactions involving multiple solvent molecules, the energies of both **2^{Fe}** and **2^{Co}** (Figure 4) were also estimated using MKM. These values were found to lie within the boundaries defined by the implicit and hybrid solvation approaches (see Supporting Information for details), providing additional validation.

Importantly, the relative stabilities of **II^M** and **2^M** provide a basis for understanding the divergent experimental behaviors observed for iron and cobalt regarding the C–H metalation of the second equivalent of pentafluorobenzene. The lower stability of **II^{Co}** coupled with the more favorable formation of the dimer **2^{Co}** compared to the iron analogues, restricts the presence of **II^{Co}** in kinetically efficient concentrations, even in THF solution. In contrast, the reversible **2^{Fe} ⇌ II^{Fe}** equilibrium plays a pivotal role in facilitating the interaction with the second equivalent of C₆F₅H (**II^{Fe}**). This interaction eventually leads to the metalated intermediate **II^{Fe}**, characterized by two Fe–C₆F₅ bonds and a protonated TMP(H) group. The formation of **II^{Fe}** is energetically favorable by –11.6 kcal mol⁻¹, requiring a relative energy barrier of 20.5 kcal mol⁻¹ (**TS2^{Fe}**) from **II^{Fe}**.

Unlike **TS1^{Fe}**, featuring a pseudo-linear geometry with two TMP ligands and a dissociated THF molecule, **TS2^{Fe}** displays a tricoordinate iron center with a bound THF molecule ([Fe(C₆F₅)(THF)(TMP)]). The linear alternative for **TS2^{Fe}** (without coordinated THF) was also considered, resulting in an energy difference of +6.5 kcal mol⁻¹ higher (Figure S87). This discrepancy in coordination between **TS1^{Fe}** and **TS2^{Fe}** can be attributed to the loss of strong donation from the spectator TMP ligand present in **TS1^{Fe}** (Fe–N = 1.832 Å), which electronically compensates for the lack of interaction with the THF molecule.

From **II^{Fe}**, the subsequent dissociation of the protonated TMP(H) and the coordination of the second THF molecule result in the formation of the reaction product [(THF)₂Fe(C₆F₅)₂] (**II^{Fe}-THF**). Overall, the formation of this product is thermodynamically favorable by –16.8 kcal mol⁻¹ (Figure 4), in line with its isolation in experiments. These computational findings are further consistent with the monobasic behavior of **II^{Fe}** observed in benzene, leading to the quantitative formation of the dimeric complex **2^{Fe}**.

Notably, in the absence of THF, the deprotonation of a second equivalent of pentafluorobenzene, directly promoted by **2^{Fe}**, was confirmed to be unfeasible ($\Delta G^\ddagger = +37.6$ and +38.7 kcal mol⁻¹ for monomeric and dimeric TSs, respec-

tively; see Figure S88). Hence, the presence of THF provides unique access to the monomeric active species $\mathbf{1}^{\text{Fe}}$, facilitating the second metalation of pentafluorobenzene. A similar behavior was not observed for cobalt due to the higher stability of the dimer $\mathbf{2}^{\text{Co}}$, increasing the overall barrier for the putative formation of $\mathbf{4}^{\text{Co}}\text{-THF}$ to $+35.9\text{ kcal mol}^{-1}$ (Figure S89). It is also noteworthy that cooperative ligand scrambling involving $\text{C}_6\text{F}_5/\text{TMP}$ exchanges was computationally proposed and experimentally verified when working with a THF solution of $\mathbf{2}^{\text{Fe}}$ in the absence of arene, resulting in mixtures containing $\mathbf{4}^{\text{Fe}}\text{-THF}$ and $\mathbf{1}^{\text{Fe}}\text{-THF}$ (Figures S33, S34 and S90).

Previous studies assessing the reactivity of Mg and Zn compounds containing TMP groups have revealed that the presence of inorganic salts, in particular LiCl can greatly enhance their kinetic basicity by forming ate complexes.^[37] This prompted us to consider a similar strategy for the transition metal amides $\mathbf{1}^{\text{Fe}}$ and $\mathbf{1}^{\text{Co}}$. In probing this, we found by spectroscopic analysis that addition of one equivalent of LiCl to d_8 -THF solutions of these complexes is accompanied with a significant shifting of the TMP resonances which are now significantly more shielded. For example, for $\mathbf{1}^{\text{Fe}}$ on addition of LiCl the TMP signals appear at 102.6, 75.70 and -5.40 ppm (vs 150.29, 110.10 and 3.82 ppm for $\mathbf{1}^{\text{Fe}}$). Moreover, its $^7\text{Li}\{^1\text{H}\}$ NMR spectrum revealed a very shifted resonance at 69.10 ppm. A similar trend was found for cobalt (see Supporting Information for details). These findings support the formation of lithium metal(ate) complexes (Figure 5). Note that the relevant co-complexes of LiCl with $\text{M}(\text{HMDS})_2$ have previously been prepared and structurally characterized.^[38] While we could not grow suitable crystals for X-crystallographic analysis using LiCl, we noticed that addition of the THF-soluble ammonium salt $(n\text{Bu})_4\text{NCl}$ to $\mathbf{1}^{\text{Fe}}$ and $\mathbf{1}^{\text{Co}}$ in THF afforded ate complexes with the TMP resonances appearing at almost identical shifts to those observed when LiCl was added. In the case of Fe, suitable crystals of the ammonium ferrate $[\{\text{NBu}_4\}\{\text{Fe}(\text{TMP})_2\text{Cl}\}]$ ($\mathbf{5}^{\text{Fe}}$) could be obtained in a 77% yield. X-ray crystallographic analysis confirmed formation of a ferrate anion resulting from co-complexation of $\text{Fe}(\text{TMP})_2$ with a Cl^- anion (Figure 5). This structure is reminiscent of

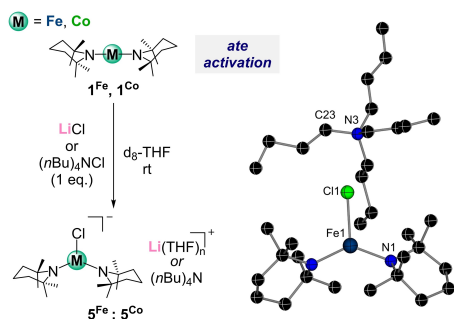


Figure 5. Ate activation by co-complexation of $\mathbf{1}^{\text{M}}$ with equimolar amounts of LiCl or NBu_4Cl in d_8 -THF. Inset: molecular structure of $\mathbf{5}^{\text{Fe}}$ displayed as a ball and stick model. Hydrogen atoms omitted for clarity.

one recently reported by Werncke for co-complexation of $(n\text{Bu})_4\text{NBr}$ with $\text{Fe}(\text{HMDS})_2$.^[39]

To test the metalating ability of these ate-activated metal amide complexes, we studied first on the reaction of $\mathbf{1}^{\text{Co}}$ with two equivalents of pentafluorobenzene. Gratifyingly on the addition of one equivalent of LiCl or $(n\text{Bu})_4\text{NCl}$ the activation of the second TMP group was proven by ^1H NMR (SI for details). While attempts to crystallize a putative $[\{\text{A}\}\{\text{Co}(\text{C}_6\text{F}_5)_2\text{Cl}\}]$ ($\text{A} = \text{Li}(\text{THF})_x^+$ or $(n\text{Bu})_4\text{N}^+$) intermediate failed, addition of NHC $t\text{Bu}$, once the metalation had occurred, led to the crystallization of $[\text{tBuCo}(\text{C}_6\text{F}_5)_2]$ ($\mathbf{4}^{\text{Co}}\text{-tBu}$) in an 82% yield (Figure 6). $\mathbf{4}^{\text{Co}}\text{-tBu}$ was characterized by X-ray crystallography as well as by ^1H and $^{19}\text{F}\{^1\text{H}\}$ NMR spectroscopy (see Figure 6 and Supporting Information for details).

Next, we tested these reaction conditions with less activated fluoroarene substrates (in terms of pK_a values) focusing on 1,3-difluorobenzene and ethyl 3-fluorobenzoate. While $\mathbf{1}^{\text{Co}}$ showed no reactivity, with $\mathbf{1}^{\text{Fe}}$ one TMP ligand reacted to give dimeric $[\{\text{Fe}(\text{TMP})\text{Ar}^{\text{F}}\}]_2$ ($\text{Ar}^{\text{F}} = 2\text{-F-6-(CO}_2\text{Et)}\text{C}_6\text{H}_3$, $\mathbf{6}^{\text{Fe}}$; $2,6\text{-F}_2\text{C}_6\text{H}_3$, $\mathbf{7}^{\text{Fe}}$) in 54 and 76% isolated yields. Remarkably, while the presence of LiCl [or NBu_4Cl] is required to promote ferration of these substrates, these additives are not incorporated in the isolated products (Figure 6). A possible explanation could be that initially $[\{\text{A}\}\{\text{Fe}(\text{TMP})(\text{Ar}^{\text{F}})\text{Cl}\}]$ ($\text{A} = \text{Li}(\text{THF})_x^+$ or NBu_4^+) ate species form, which can be in equilibrium with $[\text{Fe}(\text{TMP})(\text{Ar}^{\text{F}})]$ and LiCl [or $(n\text{Bu})_4\text{NCl}$]. This equilibrium can be shifted towards the formation of the neutral species, driven by the preferred dimerization of $[\text{Fe}(\text{TMP})(\text{Ar}^{\text{F}})]$ to give $\mathbf{6}^{\text{Fe}}$ and $\mathbf{7}^{\text{Fe}}$ respectively, especially when considering that these compounds were recrystallized from non-polar benzene (see Supporting Information for details). The structures of $\mathbf{6}^{\text{Fe}}$

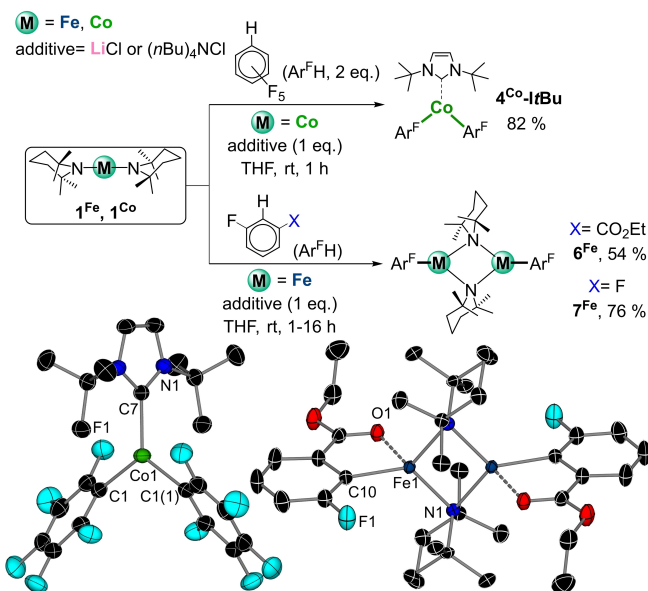


Figure 6. Reactivity of $\mathbf{1}^{\text{Fe}}$ and $\mathbf{1}^{\text{Co}}$ in the presence of LiCl or $(n\text{Bu})_4\text{NCl}$ (1 eq.). Inset: molecular structure of $\mathbf{4}^{\text{Co}}\text{-tBu}$ (left) and $\mathbf{6}^{\text{Fe}}$ (right). H atoms omitted for clarity and displacement ellipsoids displayed at 50% probability level.

and 7^{Fe} were established by X-ray crystallographic studies and the compounds were also characterized by ^1H and ^{19}F NMR spectroscopy. They exhibit similar structural and spectroscopic features to those previously described for 2^{Fe} and 3^{Fe} with the exception that for 6^{Fe} the iron center achieves further coordinative saturation by interacting with the O of the C=O substituent *ortho* to the C that has experienced ferration [Fe1-O1 , 2.296(9) Å].

Extending the applications of 1^{Fe} and 1^{Co} beyond fluoroarene metalation, we then studied whether these metal amides could also promote the deprotonation of cyclopentadiene as an alternative route to access the classical organometallic sandwich compounds, ferrocene and cobaltocene. Strikingly, ^1H NMR monitoring of the reactions in deuterated toluene showed that 1^{Fe} and 1^{Co} react at room temperature with two equivalents of freshly distilled cyclopentadiene to furnish ferrocene and cobaltocene respectively in quantitative yields with concomitant release of two equivalents of TMP(H). We also tested whether cobaltocene could be synthesized from an in situ made $\text{Co}(\text{TMP})_2$. Pleasingly, the addition of 2 equivalents of cyclopentadiene to a d_8 -toluene solution of a mixture of LiTMP (2 equivalents) and CoCl_2 resulted in an immediate color change of the solution, with the instantaneous formation of Cp_2Co (Figure 7) as witnessed by a diagnostic signal at -51.74 ppm.

In addition, the TMP groups on 1^{Fe} and 1^{Co} show excellent nucleophilicity, being able to insert two equivalents of CO_2 under mild reaction conditions affording bis(carbamate) complexes $[(\text{TMEDA})\text{M}(\text{OC}(=\text{O})\text{TMP})_2]$ (8^{Fe} , 62 % and 8^{Co} 75 % yield). Monomers 8^{Fe} and 8^{Co} feature one divalent metal coordinated to two chelating carbamate ligands via their O atoms and one TMEDA chelate, achieving a distorted octahedral geometry (Figure 7 and SI). Interestingly, the insertion process is significantly faster for Fe than Co, with full conversion to 8^{Co} over 16 hours compared to 2 hours for formation of 8^{Fe} . This reactivity is reminiscent to that previously reported by Mulvey for main group metal amides LiTMP or $\text{Al}(\text{TMP})_2\text{iBu}_2$.^[40] It should

also be noted that transition metal amide complexes can also undergo CO_2 insertion in their M–N bonds^[41] although this reactivity has been significantly less explored than those involving M–H^[42] and M–OR (R = alkyl, aryl) bonds.^[43]

Conclusion

Popular in main group chemistry, TMP complexes have been made here with the earth-abundant transition metals Fe and Co and structurally, spectroscopically, and magnetically characterized. Mimicking the reactivity of main-group metal TMPs, these metal (II) amides can promote direct ferration (or cobaltation) of fluoroarenes, without changing their oxidation state or cleaving the C–F bonds of perfluorinated substrates. Their kinetic reactivity can be boosted further by using LiCl or NBu_4Cl as additives facilitating formation of more reactive metal(ate) species. The integration of DFT calculations has enriched our mechanistic understanding, revealing nuanced differences between $\text{Fe}(\text{TMP})_2$ and $\text{Co}(\text{TMP})_2$ in their ability to act as bases using one or two of their basic arms. Additionally, we highlight the pivotal role played by the coordinating solvent THF in promoting the polybasicity of $\text{Fe}(\text{TMP})_2$.

Expanding their synthetic scope, these complexes demonstrate the ability to directly metalate cyclopentadiene, providing an alternative route to the classical organometallic sandwich complexes ferrocene and cobaltocene in quantitative yields. Furthermore, despite the steric bulk of the TMP groups, these metal amides can efficiently insert two equivalents of CO_2 under mild reaction conditions, showcasing their versatility.

Overall, this work transcends the boundaries of main group metal chemistry, unlocking new opportunities for deprotonative metalation. Their redox potential along with the more covalent character of the newly formed M–C bonds opens up a wealth of new opportunities for arene functionalization that are currently under investigation in our groups.

Acknowledgements

The X-ray crystal structure service unit at the University of Bern is acknowledged for measuring, solving, refining, and summarizing the structures of compounds 1^{Fe} , 1^{Co}-THF , $1^{\text{Co}}\text{-IMes}$, 2^{Fe} , 2^{Co} , 3^{Fe} , 3^{Co} , 4^{Fe}-THF , $4^{\text{Fe}}\text{-TMEDA}$, 4^{Co}-iBu , 5^{Fe} , 6^{Fe} , 7^{Fe} , 8^{Fe} .^[44] We are also grateful to the Swiss National Science Foundation (SNF) (projects numbers 206021_177033 and 188573), the University of Bern, the Irish Research Council (GOIPG/2021/88, M.M.), and the University of Valladolid (CONVREC-2021-221, M.N.P.-D.) for their generous sponsorship. The DJEI/DES/SFI/HEA Irish Centre for High-End Computing (ICHEC) is also acknowledged for the generous provision of computational resources. We also thank Professor Robert E. Mulvey (University of Strathclyde) for insightful discussions. Open Access funding provided by Universität Bern.

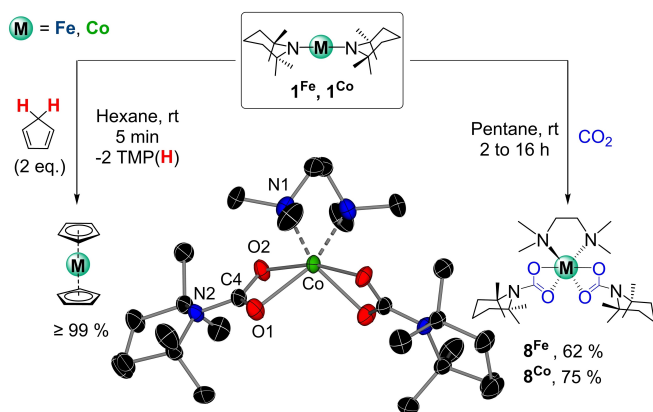


Figure 7. Reactivity of 1^{Fe} and 1^{Co} with cyclopentadiene and CO_2 . Inset: molecular structure of $[(\text{TMEDA})\text{Co}(\text{OC}(=\text{O})\text{TMP})_2]$ (8^{Co}). H atoms omitted for clarity and displacement ellipsoids displayed at 50% probability level.

Conflict of Interest

The authors declare no conflict of interest.

Data Availability Statement

The data that support the findings of this study are available in the supplementary material of this article.

Keywords: amide · cobalt · fluoroarenes · iron · metalation

- [1] a) A. S. Michael Lappert, Andrey Protchenko, Philip P. Power, *Metal Amide Chemistry*, Wiley, **2008**; b) R. E. Mulvey, S. D. Robertson, *Angew. Chem. Int. Ed.* **2013**, *52*, 11470–11487; *Angew. Chem.* **2013**, *125*, 11682–11700.
- [2] a) J. F. Remenar, B. L. Lucht, D. Kruglyak, F. E. Romesberg, J. H. Gilchirst, D. B. Collum, *J. Org. Chem.* **1997**, *62*, 5748–5754; b) E. Hevia, A. R. Kennedy, R. E. Mulvey, D. L. Ramsay, S. D. Robertson, *Chem. Eur. J.* **2013**, *19*, 14069–14075; c) M. F. Lappert, M. J. Slade, A. Singh, J. L. Atwood, R. D. Rogers, R. Shakir, *J. Am. Chem. Soc.* **1983**, *105*, 302–304; d) P. García-Álvarez, D. V. Graham, E. Hevia, A. R. Kennedy, J. Klett, R. E. Mulvey, C. T. O'Hara, S. Weatherstone, *Angew. Chem. Int. Ed.* **2008**, *47*, 8079–8081; *Angew. Chem.* **2008**, *120*, 8199–8201; e) W. Lin, O. Baron, P. Knochel, *Org. Lett.* **2006**, *8*, 5673–5676.
- [3] a) R. E. Mulvey, F. Mongin, M. Uchiyama, Y. Kondo, *Angew. Chem. Int. Ed.* **2007**, *46*, 3802–382; *Angew. Chem.* **2007**, *119*, 3876–3899; b) E. Nagaradja, F. Chevallier, T. Roisnel, V. Jouikov, F. Mongin, *Tetrahedron* **2012**, *68*, 3063–3073.
- [4] a) Y. Kondo, M. Shilai, M. Uchiyama, T. Sakamoto, *J. Am. Chem. Soc.* **1999**, 3539–3540; b) M. Uchiyama, Y. Matsumoto, D. Nobuto, T. Furuyama, K. Yamaguchi, K. Morokuma, *J. Am. Chem. Soc.* **2006**, *128*, 8748–8750; c) W. Clegg, S. H. Dale, E. Hevia, G. W. Honeyman, R. E. Mulvey, *Angew. Chem. Int. Ed.* **2006**, *45*, 2370–2374; *Angew. Chem.* **2006**, *118*, 2430–243; d) E. Hevia, D. J. Gallagher, A. R. Kennedy, R. E. Mulvey, C. T. O'Hara, C. Talmard, *Chem. Commun.* **2004**, *21*, 2422–2423; e) P. C. Andrikopoulos, D. R. Armstrong, D. V. Graham, E. Hevia, A. R. Kennedy, R. E. Mulvey, C. T. O'Hara, C. Talmard, *Angew. Chem. Int. Ed.* **2005**, *44*, 3459–3462; *Angew. Chem.* **2005**, *117*, 3525–3528; f) D. R. Armstrong, A. R. Kennedy, R. E. Mulvey, R. B. Rowlings, *Angew. Chem. Int. Ed.* **1999**, *38*, 131–133; *Angew. Chem.* **1999**, *111*, 231–233; g) M. Uchiyama, H. Naka, Y. Matsumoto, T. Ohwada, *J. Am. Chem. Soc.* **2004**, *126*, 10526–10527.
- [5] S. D. Robertson, M. Uzelac, R. E. Mulvey, *Chem. Rev.* **2019**, *119*, 8332–8405.
- [6] D. R. Armstrong, J. A. Garden, A. R. Kennedy, S. M. Leenhouts, R. E. Mulvey, P. O'Keefe, C. T. O'Hara, A. Steven, *Chem. A Eur. J.* **2013**, *19*, 13492–13503.
- [7] S. H. Wunderlich, P. Knochel, *Angew. Chem. Int. Ed.* **2009**, *48*, 9717–9720; *Angew. Chem.* **2009**, *121*, 9897–9900.
- [8] G. Dayaker, F. Chevallier, P. C. Gros, F. Mongin, *Tetrahedron* **2010**, *66*, 8904–8910.
- [9] a) H. Bürger, U. Wannagat, *Monatsh. Chem. verw. Teile anderer Wissensch.* **1963**, *94*, 1007–1012; b) R. A. Andersen, K. Faegri, J. C. Green, A. Haaland, M. F. Lappert, W. P. Leung, K. Rypdal, *Inorg. Chem.* **1988**, *27*, 1782–1786.
- [10] a) A. Panda, M. Stender, M. M. Olmstead, P. Klavins, P. P. Power, *Polyhedron* **2003**, *22*, 67–73; b) W. Alexander Merrill, T. A. Stich, M. Brynda, G. J. Yeagle, J. C. Fettinger, R. De Hont, W. M. Reiff, C. E. Schulz, R. D. Britt, P. P. Power, *J. Am. Chem. Soc.* **2009**, *131*, 12693–12702; c) W. Stroek, M. Keilwerth, D. M. Pividori, K. Meyer, M. Albrecht, *J. Am. Chem. Soc.* **2021**, *143*, 20157–20165; d) M. A. Putzer, B. Neumüller, K. Dehnicke, J. Magull, *Chem. Ber.* **1996**, *129*, 715–719; e) H. Hope, M. M. Olmstead, B. D. Murray, P. P. Power, *J. Am. Chem. Soc.* **1985**, *107*, 712–713; f) A. M. Bryan, G. J. Long, F. Grandjean, P. P. Power, *Inorg. Chem.* **2013**, *52*, 12152–12160; g) R. A. Layfield, J. J. W. McDouall, M. Scheer, C. Schwarzmaier, F. Tuna, *Chem. Commun.* **2011**, *47*, 10623–10625; h) B. M. Day, T. Pugh, D. Hendriks, C. F. Guerra, D. J. Evans, F. M. Bickelhaupt, R. A. Layfield, *J. Am. Chem. Soc.* **2013**, *135*, 13338–13341; i) L. C. H. Maddock, T. Cadenbach, A. R. Kennedy, I. Borilovic, G. Aromí, E. Hevia, *Inorg. Chem.* **2015**, *54*, 9201–9210; j) A. Massard, P. Braunstein, A. A. Danopoulos, S. Choua, P. Rabu, *Organometallics* **2015**, *34*, 2429–2438; k) R. Araake, K. Sakadani, M. Tada, Y. Sakai, Y. Ohki, *J. Am. Chem. Soc.* **2017**, *139*, 5596–5606; l) T. N. Gieshoff, U. Chakraborty, M. Villa, A. Jacobi von Wangelin, *Angew. Chem. Int. Ed.* **2017**, *56*, 3585–3589; *Angew. Chem.* **2017**, *129*, 3639–3643; m) C. Y. Lin, J. C. Fettinger, F. Grandjean, G. J. Long, P. P. Power, *Inorg. Chem.* **2014**, *53*, 9400–9406.
- [11] a) B. A. Frazier, P. T. Wolczanski, E. B. Lobkovsky, T. R. Cundari, *J. Am. Chem. Soc.* **2009**, *131*, 3428–3429; b) R. A. Bartlett, J. J. Ellison, P. P. Power, S. C. Shoner, *Inorg. Chem.* **1991**, *30*, 2888–2894; c) H. Chen, M. M. Olmstead, D. C. Pestana, P. P. Power, *Inorg. Chem.* **1991**, *30*, 1783–1787; d) Y. Ohki, Y. Ikagawa, K. Tatsumi, *J. Am. Chem. Soc.* **2007**, *129*, 10457–10465.
- [12] a) L. C. H. Maddock, T. Nixon, A. R. Kennedy, M. R. Probert, W. Clegg, E. Hevia, *Angew. Chem. Int. Ed.* **2018**, *57*, 187–191; *Angew. Chem.* **2018**, *130*, 193–197; b) L. C. H. Maddock, M. Mu, A. R. Kennedy, M. García-Melchor, E. Hevia, *Angew. Chem. Int. Ed.* **2021**, *60*, 15296–15301; *Angew. Chem.* **2021**, *133*, 15424–15429; c) A. Logallo, M. Mu, M. García-Melchor, E. Hevia, *Angew. Chem. Int. Ed.* **2022**, *61*, e202213246; *Angew. Chem.* **2022**, *134*, e202213246; d) A. Logallo, E. Hevia, *Chem. Commun.* **2023**, *59*, 5383–5386.
- [13] Despite several attempts, it was not possible to prepare crystalline samples of 1^{Co} suitable for X-ray crystallographic studies. 1^{Co} and 1^{Co} -THF were fully characterized in C_6D_6 solution by 1H NMR spectroscopy, see Supporting Information for details.
- [14] W. S. Rees, O. Just, H. Schumann, R. Weimann, *Polyhedron* **1998**, *17*, 1001–1004.
- [15] D. R. Armstrong, A. R. Kennedy, R. E. Mulvey, J. A. Parkinson, S. D. Robertson, *Chem. Sci.* **2012**, *3*, 2700–2707.
- [16] P. P. Power, *Chem. Rev.* **2012**, *112*, 3482–3507.
- [17] A. M. Bryan, G. J. Long, F. Grandjean, P. P. Power, *Inorg. Chem.* **2013**, *52*, 12152–12160.
- [18] While no spectroscopic or structural evidence has been previously reported for the formation of $Fe(TMP)_2$, there are a handful of structurally defined sodium ferrates which contain TMP anions, see: a) P. Alborés, L. M. Carrella, W. Clegg, P. García-Álvarez, A. R. Kennedy, J. Klett, R. E. Mulvey, E. Rentschler, L. Russo, *Angew. Chem. Int. Ed.* **2009**, *48*, 3317–3321; *Angew. Chem.* **2009**, *121*, 3367–3371.
- [19] a) P. P. Power, *Chem. Rev.* **2012**, *112*, 3482–3507; b) J. M. Zdrozny, D. J. Xiao, M. Atanasov, G. J. Long, F. Grandjean, F. Neese, J. R. Long, *Nat. Chem.* **2013**, *5*, 577–581; c) P. C. Bunting, M. Atanasov, E. Damgaard-Moller, M. Perfetti, I. Crassee, M. Orlita, J. Overgaard, J. van Slageren, F. Neese, J. R. Long, *Science* **2018**, *362*, eaat7319.
- [20] a) W. M. Reiff, A. M. LaPointe, E. H. Witten, *J. Am. Chem. Soc.* **2004**, *126*, 10206–10207; b) W. M. Reiff, C. E. Schulz, M.-H. Whangbo, J. I. Seo, Y. S. Lee, G. R. Potratz, C. W. Spicer, G. S. Girolami, *J. Am. Chem. Soc.* **2009**, *131*, 404–405; c) J. M. Zdrozny, M. Atanasov, A. M. Bryan, C.-Y. Lin, B. D.

- Rekken, P. P. Power, F. Neese, J. R. Long, *Chem. Sci.* **2013**, *4*, 125–138.
- [21] a) J. Cheng, J. Liu, X. Leng, T. Lohmiller, A. Schnegg, E. Bill, S. Ye, L. Deng, *Inorg. Chem.* **2019**, *58*, 7634–7644; b) J. M. Zadrozny, D. J. Xiao, J. R. Long, M. Atanasov, F. Neese, F. Grandjean, G. J. Long, *Inorg. Chem.* **2013**, *52*, 13123–13131.
- [22] a) C. G. Werncke, P. C. Bunting, C. Duhayon, J. R. Long, S. Bontemps, S. Sabo-Etienne, *Angew. Chem. Int. Ed.* **2015**, *54*, 245–248; *Angew. Chem.* **2015**, *127*, 247–250; b) R. Weller, M. Atanasov, S. Demeshko, T.-Y. Chen, I. Mohelsky, E. Bill, M. Orlika, F. Meyer, F. Neese, C. G. Werncke, *Inorg. Chem.* **2023**, *62*, 3153–3161.
- [23] a) C. Ni, T. A. Stich, G. J. Long, P. P. Power, *Chem. Commun.* **2010**, *46*, 4466–4468; b) A. M. Bryan, W. A. Merrill, W. M. Reiff, J. C. Fettinger, P. P. Power, *Inorg. Chem.* **2012**, *51*, 3366–3373; c) X.-N. Yao, J.-Z. Du, Y.-Q. Zhang, X.-B. Leng, M.-W. Yang, S.-D. Jiang, Z.-X. Wang, Z.-W. Ouyang, L. Deng, B.-W. Wang, S. Gao, *J. Am. Chem. Soc.* **2017**, *139*, 373–380.
- [24] K. Shen, Y. Fu, J. N. Li, L. Liu, Q. X. Guo, *Tetrahedron* **2007**, *63*, 1568–1576.
- [25] a) O. Eisenstein, J. Milani, R. N. Perutz, *Chem. Rev.* **2017**, *117*, 8710–8753; b) N. Judge, A. Logallo, E. Hevia, *Chem. Sci.* **2023**, 11617–11628.
- [26] The high solubility of these compounds in pentane led to relatively modest yields for the crystalline products but NMR analysis of the reaction filtrate are consistent with their selective formation in quantitative yields.
- [27] a) H. Müller, W. Seidel, H. Görls, *J. Organomet. Chem.* **1994**, *472*, 215–220; b) A. Klose, E. Solari, C. Floriani, A. Chiesi-Villa, C. Rizzoli, N. Re, *J. Am. Chem. Soc.* **1994**, *116*, 9123–9135; c) S. Yogendra, T. Weyhermüller, A. W. Hahn, S. Debeur, *Inorg. Chem.* **2019**, *58*, 9358–9367; d) K. H. Theopold, J. Silvestre, E. K. Byrne, D. S. Richeson, *Organometallics* **1989**, *8*, 2001–2009; e) R. A. Lewis, S. Morochnik, A. Chapovetsky, G. Wu, T. W. Hayton, *Angew. Chem. Int. Ed.* **2012**, *51*, 12772–12775; *Angew. Chem.* **2012**, *124*, 12944–12947.
- [28] For a selection of examples see: a) T. Zheng, J. Li, S. Zhang, B. Xue, H. Sun, X. Li, O. Fuhr, D. Fenske, *Organometallics* **2016**, *35*, 3538–3545; b) J. Vela, J. M. Smith, Y. Yu, N. A. Ketterer, C. J. Flaschenriem, R. J. Lachicotte, P. L. Holland, *J. Am. Chem. Soc.* **2005**, *127*, 7857–7870; c) J. Li, T. Zheng, H. Sun, W. Xu, X. Li, *Dalton Trans.* **2013**, *42*, 5740–5748; d) T. R. Dugan, J. M. Goldberg, W. W. Brennessel, P. L. Holland, *Organometallics* **2012**, *31*, 1349–1360; e) T. P. Pabst, J. V. Obligation, É. Rochette, I. Pappas, P. J. Chirik, *J. Am. Chem. Soc.* **2019**, *141*, 15378–15389; f) T. P. Pabst, P. J. Chirik, *Organometallics* **2021**, *40*, 813–831; g) I. Müller, C. G. Werncke, *Chem. Eur. J.* **2021**, *27*, 4932–4938.
- [29] a) M. Mosrin, P. Knochel, *Org. Lett.* **2009**, *11*, 1837–1840; b) P. Mastropierro, A. R. Kennedy, E. Hevia, *Chem. Commun.* **2022**, *58*, 5292–5295; c) N. R. Judge, E. Hevia, *Angew. Chem. Int. Ed.* **2023**, *62*, e20230309; *Angew. Chem.* **2023**, *135*, e2023030; d) R. McLellan, M. Uzelac, A. R. Kennedy, E. Hevia, R. E. Mulvey, *Angew. Chem. Int. Ed.* **2017**, *56*, 9566–9570; *Angew. Chem.* **2017**, *129*, 9694–9698.
- [30] a) N. J. Bakas, J. D. Sears, W. W. Brennessel, M. L. Neidig, *Angew. Chem. Int. Ed.* **2022**, *61*, e202114986; *Angew. Chem.* **2022**, *134*, e202114986; b) D. Noda, Y. Sunada, T. Hatakeyama, M. Nakamura, H. Nagashima, *J. Am. Chem. Soc.* **2009**, *131*, 6078–6079.
- [31] a) R. J. Wehmschulte, P. P. Power, *Organometallics* **1995**, *239*, 39–42; b) D. L. Kays, A. R. Cowley, *Chem. Commun.* **2007**, *58*, 1053–1055; c) C. Ni, P. P. Power, *Chem. Commun.* **2009**, 5543–5545.
- [32] For a related titration experiment of Fe and Co(II) bis(amides) see: C. Y. Lin, J. C. Fettinger, P. P. Power, *Inorg. Chem.* **2017**, *56*, 9892–9902.
- [33] M. Manting, M. N. Peñas-Defrutos, M. García-Melchor, *Adv. Coord. Chem. in press*, doi.org/10.1016/bs.adomc.2024.03.001.
- [34] a) M. F. Bickelhaupt, *J. Comput. Chem.* **1999**, *20*, 114–128; b) M. García-Melchor, S. I. Gorelsky, T. K. Woo, *Chem. A Eur. J.* **2011**, *17*, 13847–13853; c) M. Mu, A. Logallo, E. Hevia, M. García-Melchor, *ChemCatChem* **2023**, *15*, e202300769.
- [35] All the DFT data underlying this work, including the Cartesian coordinates and energies of all the modeled structures, is openly accessible via the following ioChem-BD online dataset: <https://doi.org/10.19061/iochem-bd-6-327>
- [36] C. L. McMullin, J. Jover, J. N. Harvey, N. Fey, *Dalton Trans.* **2010**, *39*, 10833–10836.
- [37] a) A. Krasovskiy, V. Krasovskaya, P. Knochel, *Angew. Chem. Int. Ed.* **2006**, *45*, 2958–2961; *Angew. Chem.* **2006**, *118*, 3024–3027; b) G. C. Clososki, C. J. Rohbogner, P. Knochel, *Angew. Chem. Int. Ed.* **2007**, *46*, 7681–7684; *Angew. Chem.* **2007**, *119*, 7825–7827; c) C. Feng, D. W. Cunningham, Q. T. Easter, S. A. Blum, *J. Am. Chem. Soc.* **2016**, *138*, 11156–11159.
- [38] U. Siemeling, U. Vorfeld, B. Neumann, H. G. Stammer, *Inorg. Chem.* **2000**, *39*, 5159–5160.
- [39] R. Weller, L. Völlinger, C. G. Werncke, *Eur. J. Inorg. Chem.* **2021**, 4383–4392.
- [40] A. R. Kennedy, R. E. Mulvey, D. E. Oliver, S. D. Robertson, *Dalton Trans.* **2010**, *39*, 6190–6197.
- [41] a) N. Hazari, J. E. Heimann, *Inorg. Chem.* **2017**, *56*, 13655–13678; b) J. E. Heimann, W. H. Bernskoetter, J. A. Guthrie, N. Hazari, J. M. Mayer, *Organometallics* **2018**, *37*, 3649–3653.
- [42] For selected references see: a) L. D. Field, E. T. Lawrenz, W. J. Shaw, P. Turner, *Inorg. Chem.* **2000**, *39*, 5632–5638; b) L. D. Field, W. J. Shaw, P. Turner, *Chem. Commun.* **2002**, *2*, 46–47; c) O. R. Allen, S. J. Dalgarno, L. D. Field, *Organometallics* **2008**, *27*, 3328–3330; d) Y. Zhang, A. D. MacIntosh, J. L. Wong, E. A. Bielinski, P. G. Williard, B. Q. Mercado, N. Hazari, W. H. Bernskoetter, *Chem. Sci.* **2015**, *6*, 4291–4299; e) U. Jayarathne, N. Hazari, W. H. Bernskoetter, *ACS Catal.* **2018**, *8*, 1338–1345; f) L. S. Pu, A. Yamamoto, S. Ikeda, *J. Am. Chem. Soc.* **1968**, *90*, 3896; g) M. L. Scheuermann, S. P. Semproni, I. Pappas, P. J. Chirik, *Inorg. Chem.* **2014**, *53*, 9463–9465; h) S. R. Tamang, M. Findlater, *Dalton Trans.* **2018**, *47*, 8199–8203; i) J. E. Heimann, W. H. Bernskoetter, N. Hazari, *J. Am. Chem. Soc.* **2019**, *141*, 10520–10529; j) Y. Tsubonouchi, D. Takahashi, M. R. Berber, E. A. Mohamed, Z. N. Zahran, A. M. Alenad, N. A. Althubiti, M. Yagi, *Electrochim. Acta* **2021**, *387*, 138545; k) H. H. Cramer, S. Ye, F. Neese, C. Werlé, W. Leitner, *JACS Au* **2021**, *1*, 2058–2069.
- [43] For selected references see: a) O. R. Allen, S. J. Dalgarno, L. D. Field, P. Jensen, A. J. Turnbull, A. C. Willis, *Organometallics* **2008**, *27*, 2092–2098; b) W. K. Offermans, C. Bizzarri, W. Leitner, T. E. Müller, *Beilstein J. Org. Chem.* **2015**, *11*, 1340–1351; c) E. Chaffee, T. P. Dasgupta, G. M. Harris, *J. Am. Chem. Soc.* **1973**, *95*, 4169–4173.
- [44] Deposition Numbers 2314566 (for **1^{Fe}**), 2314564 (for **1^{Co}-THF**), 2314565 (for **1^{Co}-IMes**), 2314568 (for **2^{Fe}**), 2314567 (for **2^{Co}**), 22314570 (for **3^{Fe}**), 2314569 for **3^{Co}**), 2314574 (for **4^{Fe}-THF**), 2314575 (for **4^{Fe}-TMEDA**), 2314573 (for **4^{Co}-IrBu**), 2314577 (for **5^{Fe}**), 23145572 (for **6^{Fe}**), 2314571 (for **7^{Fe}**), 2314578 (for **8^{Fe}**) and 2314576 (for **8^{Co}**) contains the supplementary crystallographic data for this paper. These data are provided free of charge by the joint Cambridge Crystallographic Data Centre and Fachinformationszentrum Karlsruhe Access Structures service.

Manuscript received: February 8, 2024

Accepted manuscript online: April 2, 2024

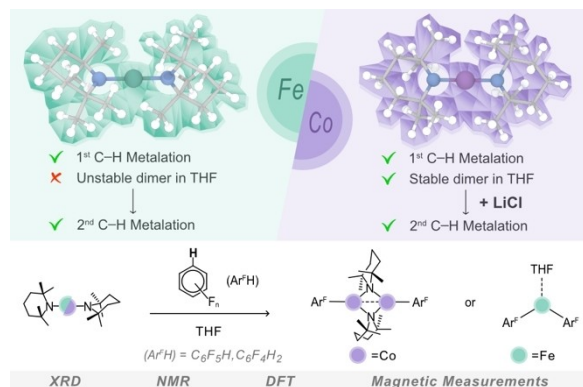
Version of record online: ■■■, ■■■

Research Articles

Fluoroarenes

A. Logallo, L. C. H. Maddock, M. Mu,
L. Gravogl, N. Jin, M. N. Peñas-Defrutos,
K. Meyer, M. García-Melchor,*
E. Hevia* [e202402907](#)

Unlocking the Metalation Applications of
TMP-powered Fe and Co(II) bis(amides):
Synthesis, Structure and Mechanistic In-
sights



Reversing the more usual trend of replicating transition metal chemistry with main group compounds, this work elaborates the applications of the new earth-abundant d-block amides Fe-

(TMP)₂ and Co(TMP)₂ in deprotonative metalation chemistry, a field dominated by highly polar s-block amides such as LiTMP and NaTMP (TMP = 2,2,6,6-tetramethylpiperide).